行政院國家科學委員會專題研究計畫 成果報告

醫用加速器的中子輻射評估
研究成果報告(精簡版)

計 畫 類 別 ： 個別型
計 畫 編 號 ： NSC 96-2320-B-040-017-
執 行 期 間 ： 96 年 08 月 01 日至 97 年 07 月 31 日
執 行 單 位 ： 中山醫學大學醫學影像暨放射科學系

計 畫 主 持 人 ： 陳健懿
共 同 主 持 人 ： 劉文山
計 畫 參 與 人 員 ： 此計畫無其他參與人員：

處 理 方 式 ： 本計畫涉及專利或其他智慧財產權，2 年後可公開查詢

中 華 民 國 97 年 08 月 14 日

行政院國家科學委員會專題研究計畫成果報告

醫用加速器的中子輻射評估

Evaluation of Neutron Radiation Dose for Medical Accelerator

1. 中文摘要

高能直線加速器(linac)產生電子及 x-光進行癌症治療，惟高出 10-MV 的加速器會經由光核反應產生巨量中子自靶區外釋，以銦片始活化法可利用產生的 $^{115}In(n,\gamma)^{116m}In$ 度量中山醫學大學附設醫院放射腫瘤科 15、10 及 6-MV 的 Varian Clinac 21Ex 醫用直線加速器中治療室之熱中子通率(Φ_{th})及估算熱中子劑量，歸因於中子受到鉛與天花板的散射及緩衝而增高，又因 6-MV 光子能量太低而無法測得 Φ_{th}。迷道的什值層(tenth-value layer (TVL))測量得到值為 XX,可證明中山醫大的 10 公分迷道設計可適用於輻射屏蔽.

關鍵字：醫用直線加速器, 什值層, 迷道設計

Abstract

The indium foil activation technique has been employed to measure thermal neutron fluences (Φ_{th}) among various locations in treatment room with a 20×20 cm^2 field size and a 15 and 10 MV x-ray beam. Spatial Φ_{th} are visualized using colored three-dimensional graphical representations. The Φ_{th} is found to increase the with x-ray energy of the linac and decrease as distance away from the beam center. However, thermal neutron exposure is not assessed in routine dosimetry planning and radiation assessment of patients. Distributions of Φ_{th} were measured in water phantom irradiated with 15 MV x-ray beams. The shielding effect of the maze was also evaluated. The experimentally estimated Φ_{th} along the maze distance was fitted explicate and the tenth-value layer (TVL) was calculated and discussed. Use of a 10-cm-thick polyethylene door placed at the maze was suitable for radiation shielding.

Keyword: linear accelerator, tenth-value layer, maze design

1. Introduction

High-energy electron accelerators, such as the electron linear accelerator (linac), are utilized routinely to generate photon beams for cancer therapy. However, when high-energy accelerators are operated at roughly 10 MV, a significant number of neutrons are generated through photonuclear reactions via (e, n) and (x, n), such that high-energy bremsstrahlung react with the target, dynamic wedge and multi-leaves resulting in a mixed radiation field in the radiotherapy area[1-4]. With growing interest in the use of high-energy photon beams at

Chung Shan Medical University Hospital (CSMUH), detailed measurements of thermal neutron fluences (Φ_{th}) are required. Thermal neutron fluences have been extensively investigated using calculations and measurement techniques for linacs with various energies. Table I lists the neutron fluences in the 10–25 MV range[1,2,5–11]. The foil activation technique has been employed for three-dimensional distribution measurements of Φ_{th}. Neutrons are, however, scattered in the human body. The neutron field in the body differs from that in the primary field. Distributions of Φ_{th} depth were measured in a water phantom irradiated with a 15 MV X-ray beam. The problem of adequate shielding from maze and neutron scattering into the maze may require additional attention. The tenth-value layer (TVL) of Φ_{th} was expressed as an exponential function to the calculated points in the maze.

2. Materials and Methods

2.1 Neutron activation of indium foils

The activation technique has been widely used for measurement of neutron fluxes and the corresponding doses (Knoll, 1989). Fast and thermal neutrons can be discriminated by irradiating appropriate foil materials and measuring the induced radioactivities (Lin et al., 2001; Paredes et al., 1999; Palta, et al., 1985; Deye and Young, 1977; Price and Holeman, 1978; Gur et al., 1987; McGinley et al., 1976; Uwamino et al., 1986). In the measurement of thermal neutrons, indium foils are commonly used due primarily to indium's high cross section and suitable half life ($t_{1/2}$=54.1m) (Reus and Westmeier, 1983). In this study, indium foils were used to contour the distribu-

tion of thermal neutrons around a medical accelerator. The thermal neutron flux is defined and determined by measuring the induced radioactivities of indium foils, as follows:

$$A = \phi_{th} \times \sigma_{In} \times N_A \times \frac{m \times a}{M} \times (1 - e^{-\lambda t_i}) \times e^{-\lambda t_c},$$

where ϕ_{th} is the thermal neutron flux (cm^{-2}•s^{-1}); σ_{In} is the cross section of the activation reaction (161 barns); N_A is the Avogadro's number (6.02 x 10^{23} in atoms per g-atom); m is the mass of indium foil (g); a the isotopic abundance of ^{115}In (95.7%); M is the atomic weight of indium (114.82); λ is the disintegration rate of ^{116m}In (2.135×10^{-4} s^{-1}); t_i is the irradiation time, and t_c is the time duration between irradiation and measurement.

2.2 The maze design of the 15-MV treatment room at CSMUH

A maze and shielded entrance slide door is utilized to protect personnel outside the facility. Point A (-3.8, -5.9, 0) is on the maze centerline and visible from the isocenter (Fig. 1). All measurements were performed by placing indium foils at locations A and B,(7.8,-5.9, 0) (near the 10 cm PE sliding door) at 0.5–1 m intervals along a straight line.

2.3 Neutron irradiation

Twenty indium foils (purity > 99.9%; 25 mm L×25 mm W×1 mm H) with an averaged mass of (4.86±0.07) g were used in the experiment. The foils were placed and distributed evenly in the vicinity of a medical accelerator (Clinac 21EX, Varian, Pelo Alto, CA) for neutron irradiation. The electron accelerator provides dual photoenergies with accelerating voltages of 6 and 15 MV. The beam intensity was controlled by changing the pulse interval. Figure 1 displays a floor plan of the radiotherapy facility.

The accelerator was operated at 15 MV for 2.5 min, delivering a dose of 1000 cGy at depth of dose maximum in a water-equivalent phantom with source-surface distance of 100 cm and the collimator open to a field size of 20×20 cm^2. For batch irradiation, all measured values were normalized to a reference foil, which was placed at the isocenter (0,0,0), which is exactly 100 cm below the x-ray target, such that the relative intensity of the thermal neutron in the treatment room can be simply described. The thermal neutron flux can be averaged by integrating thermal neutron flux with distance from the reference point.

2.4 Radioactivity measurement

The irradiated foils were immediately transferred to a gamma-ray spectrometric system, which consisted of a 30% high-purity germanium detector (GC3520, Canberra Industries, Meriden, CT, USA). The measured gamma-ray spectra were collected with a multichannel analyzer (35-Plus, Canberra Industries, Meriden, CT, USA) and were further analyzed by gamma-ray spectrum software. The foils were placed immediately on the face of the detector for counting; the efficiency was determined to be XX% at the characteristic gamma-ray energy of 417 keV emitted from the activated nuclide ^{116m1}In.

3. Results and Discussion

3.1 Thermal neutron flux distribution

The thermal neutron flux (ϕ_{th}) around the

medical accelerator in the treatment room was determined by measuring the radioactivities of the indium foils and then calculated by Eq. (1). The thermal neutron flux at the linac isocenter, in the beam field, was determined to be XX$\times10^4$ cm$^{-2}\cdot$s^{-1}, which is approximately the averaged value in the beam field over an area of 20×20 cm^2. Figure 2 presents the profile of the thermal neutron flux along the X axis, varied from X$\times10^3$ to XX$\times10^4$ cm$^{-2}\cdot$s^{-1} with higher values in the beam field than outside it. Figure 3 presents the profile of the thermal neutron flux along the Y axis (0,y,0): the thermal neutron flux slightly declined with distance from the isocenter. It was remarkably shielded to under X$\times10^3$ cm$^{-2}\cdot$s^{-1} in the maze and XX$\times10^3$ cm$^{-2}\cdot$s^{-1} near the wall behind the accelerator. The thermal neutron flux between the gantry head and the ceiling was 20-50 % higher than that at the isocenter because the neutrons were scattered and moderated with the lead shield in the gantry head, as illustrated in Fig. 4. The maximal value of X.0$\times10^4$ cm$^{-2}\cdot$s^{-1} in the treatment room was measured 1.5 m above the gantry head. The thermal neutron flux was slightly raised near the ground because the neutrons were moderated by scattering in the concrete material. The thermal neutron flux, ranging from X$\times10^3$ to X$\times10^4$ cm$^{-2}\cdot$s^{-1}, seemed to be roughly uniform in the treatment room except in the maze (less than 2×10^3). Integrating the thermal neutron flux distribution relative to the reference position yields an estimate of averaged neutron flux $\overline{\phi}_{th}$ in the room, XX$\times10^4$ cm$^{-2}\cdot$s^{-1}.

Figure 5 compares the gamma-ray spectra for the irradiated indium foils placed inside and

outside the beam field. The photopeak at 336 keV in Fig. 5(a) was from ^{115m}In, and was associated mainly with high-energy photon interaction through an ^{115}In (γ,γ') ^{115m}In reaction (Chao et al., 2001).

3.2 Thermal neutron dose

According to American Association of Physicists in Medicine Task Group (AAPM) report 19, the thermal neutron dose conversion factors are 2.4 pGy min^{-1} per n cm^{-2} s^{-1}.(Lin, 2001; AAPM No 19, 1986) Therefore, based on the data. It is assumed that the radiation weighting factor is set at 5 for thermal neutrons. (NCRP, No 16. 1993)

3.3 Φ_{th} in the maze

The Φ_{th} were measured along the line A-B (cf Fig 1). The Φ_{th} at point A was equal to XX% of that at the isocenter, which was higher than that at other places in the maze due to neutrons leaking through the accelerator head. This finding states that photoneutrons are emitted strongly forward after being produced by high-energy X-rays from beam-modified devices. Figure 6 presents a semi-log plot of the Φ_{th} as function of distance (x) along the A-B centerline.

The $\Phi_{th, x}$ (Fig. 6) can be expressed as an exponential function of x:

$$\Phi_{th, x} = \Phi_{th} \cdot 10^{-TVL \cdot x} \qquad (4)$$

where $\Phi_{th, x}$ is the Φ_{th} of the x position, TVL is tenth-value layer (m) of Φ_{th} in the maze. The TVL can be obtained from Fig. 6 by extrapolating the portion of curve with a y value to a point on the A-B straight line. The TVL was estimated at XX±xx m in this study. This experimental result is > 6.4 m, as obtained by McGinly and Miner, who proposed that a TVL > 6.4 m can be classified as

hard or the high-energy component of neutrons[16]. At point "S" outside the sliding door, the Φ_{th} were negligible or below the detection limit (DL) of the indium foil activation approach, indicating that 10-cm PE effectively attenuates the penetrating neutrons and an adequate shielding design of the wall and maze (cf. Fig 1).

4. Conclusion

The neutron activation method based on foil activation technique is an effective way to measure Φ_{th} from electron medical accelerators. The results of Φ_{th} measurements on Varian clinac 21EX accelerators are shown in Fig 4, reporting Φ_{th} as a function of distance from central axis. Φ_{th} between the gantry head and the ceiling was 20-50 % higher than that at the isocenter because the neutrons were scattered and moderated with the lead shield in the gantry head. But Φ_{th} can't be measured at 6-MV due to low x-ray energy of linac.

5. Acknowledgements

References

1. Konefał A, Dybek M, Zipper W, Łobodziec W, Szczucka K. Thermal and epithermal neutrons in the vicinity of the Primus Siemens biomedical accelerator. *Nukleonika* 2005; 50(2) : 73−81.

2. Lin JP, Chua TC, Lin SY, Liu MT. The measurement of photoneutrons in the

vicinity of a Siemens Primus linear accelerator. *Appl Radiat Isot* 2001; 55 : 315–21.

3. Kase KR, Mao XS, Nelson WR, Liu JC, Kleck JH, Elsalim M. Neutron fluence and energy spectra around the varian clinac 2100C/2300C medical accelerator. *Health Phys* 1998; 74 : 38–47.

4. American Association of Physicists in Medicine. Neutron measurements around high energy X-ray radiotherapy machine. AAPM 19, 1986; New York.

5. Paredes L, Genis R, Balcazar M, Tavera L, Camacho E. Fast neutron leakage in 18 MeV Medical electron accelerator. *Radiat Meas* 1999; 31 : 475-8.

6. Palta JR, Hogstrom KR, Tannanonta C. Neutron leakage measurements from a medical accelerator. *Med Phys* 1984; 11(4) : 498-501.

7. Gur D, Rosen JC, Bukovitz AG, Gill AW. Fast and slow neutrons in an 18-MV photo beam from a Philips SL/75-20 linear accelerator. *Med Phys* 1978; 5(3) : 221-2.

8. Deye JA, Young FC. Neutron Production from 10 MV Medical Linac. *Phys Med Biol* 1977; 22 (1) : 90-4.

9. McGinley PH, Wood M, Millis M, Rodriguez R. Dose levels due to neutrons in the vicinity of high-energy medical accelerators. *Med Phys* 1976; 3(6) : 397-402.

10. Barquero R, Mendez R, Vega-Carrillo, HR, Iniguez MP, Edwards TM. NEUTRON SPECTRA AND DOSIMETRIC FEATURES AROUND AN 18 MV LINAC ACCELERATOR. *Health Phys* 2005; 88(1) : 48–58.

11. Uwamino Y, Nakamura T, Ohkubo T, Hara A. Measurement and calculation of neutron leakage from a medical electron accelerator. *Med Phys* 1986; 13(3) : 374-84.

12. Chao JH, Hsu PC, Liu HM. Measurement of high dose rates byphoton activation of indium foils. *Appl Radiat Isot* 2001; 55 : 549–56.

13. McGinley PH. Photoneutron fields in medical accelerator rooms with primary barriers constructed of concrete and metals. *Health Phys* 1992; 63(6) : 698-701.

14. Chen CY, Lin, DB, Chen WK. Elements in the sera of preschool children living in central Taiwan. *Chinese J of Chem* 2007; 25 : 515-20.

15. McCall RC. Shielding for thermal neutrons. *Med Phys* 1997; 24(1) : 135-6.

16. McGinley PH, Miner M. A Method of Eliminating the Maze Door of Medical Accelerator Rooms. *Radiat Prot Manage* 1995; 12 No.5 : 29-37.

17. Chen CY. Optimal conditions for identifying ^{80}Br and ^{128}I in health food Angelica keiskei using rapid epithermal neutron activation analysis. *Appl Radiat Isot* 2003; 58(4) : 423-9.

18. Currie LA. Limits for Qualitative Detection and Quantitative Determination. *Anal Chem* 1968; 40 : 586-93.
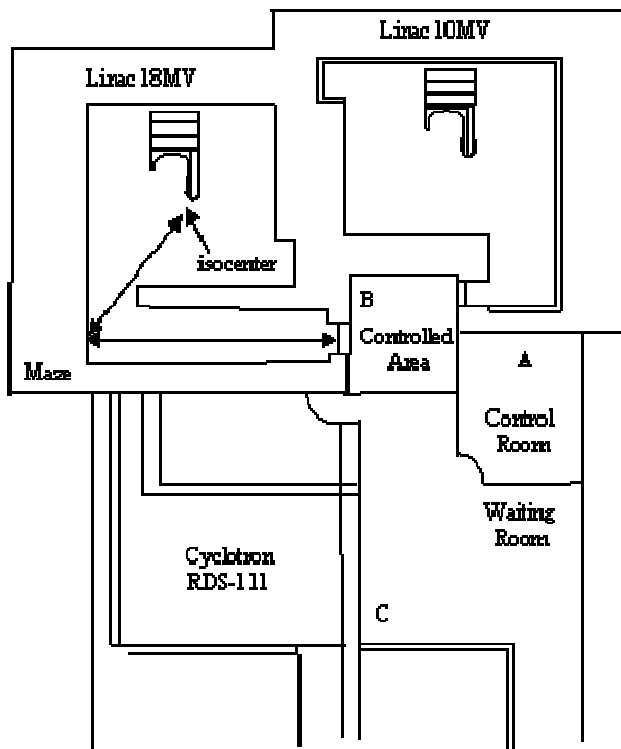
Figure 1. Plane view and measurement locations in the Varian Clinac 21EX treatment room at CSMUH. The 10-cm-thick PE sliding door was installed to decrease transmitted neutron fluence. Figure 1. Plane view and measurement locations in the Varian Clinac 21EX treatment room at CSMUH. The 10-cm-thick PE sliding door was installed to decrease transmitted neutron fluence.
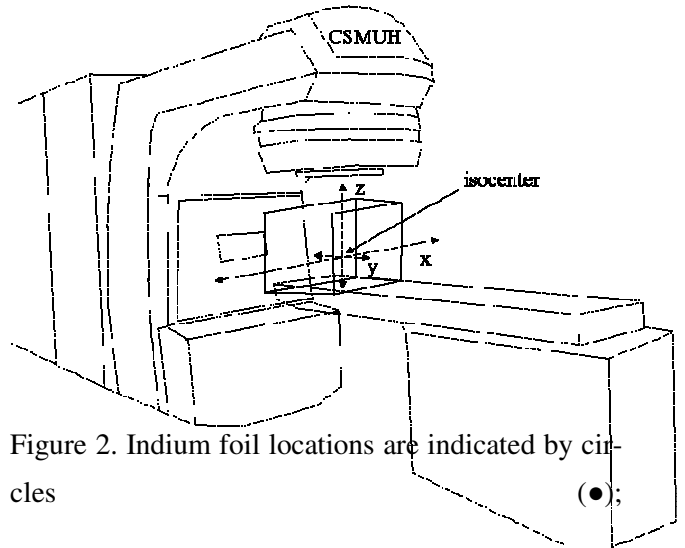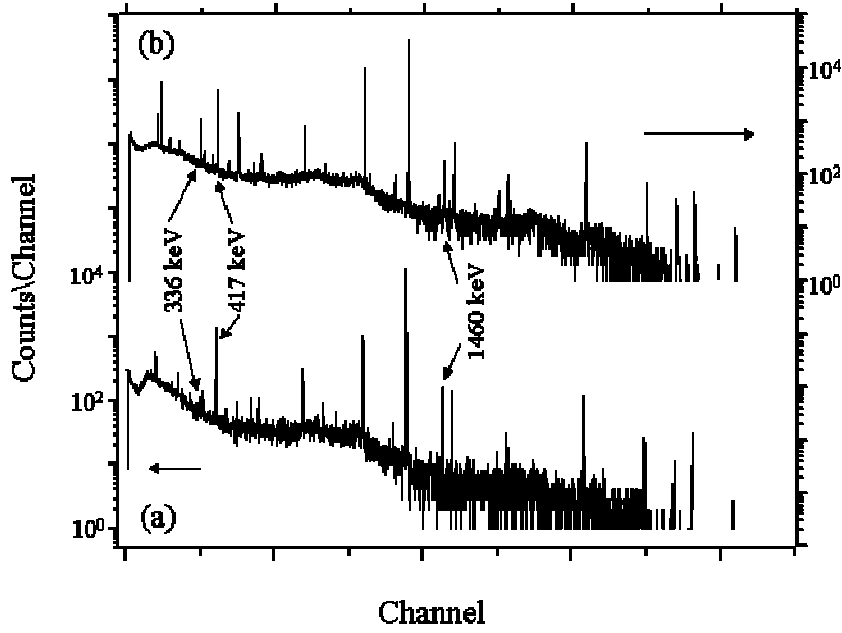
.

Figure 2. Indium foil locations are indicated by circles (●);

(a) the x and y axes correspond to locations in the treatment room for SSD=100 cm for 15 and 10 MV X-ray exposures, respectively; (b) measurements of Φ_{th} performed in the water phantom] during exposure to 15 MV X-rays.

Figure 6.

Figure 6. The exponential fitting curves of Φ_{th} in the maze. Locations of the Φ_{th} estimation (A-B) points are shown with the corresponding distances from the maze entrance.